Hindawi
Laser and Particle Beams
Volume 2022, Article ID 9868807, 7 pages
https://doi.org/10.1155/2022/9868807

Research Article

Laser-Driven Proton-Boron Fusions: Influences of the Boron State

Xiaochuan Ning,[1] **Tianyi Liang**,[1] **Dong Wu**,[2] **Shujun Liu**,[1] **Yangchun Liu**,[1] **Tianxing Hu**,[1] **Zhengmao Sheng**,[1] **Jieru Ren**,[3] **Bowen Jiang**,[4] **Yongtao Zhao**,[3] **Dieter H. H. Hoffmann**,[3] **and X.T. He**[1]

[1]*Institute for Fusion Theory and Simulation, Department of Physics, Zhejiang University, Hangzhou 310027, China*
[2]*Key Laboratory for Laser Plasmas and School of Physics and Astronomy, and Collaborative Innovation Center of IFSA (CICIFSA), Shanghai Jiao Tong University, Shanghai 200240, China*
[3]*MOE Key Laboratory for Nonequilibrium Synthesis and Modulation of Condensed Matter, School of Physics, Xi'an Jiaotong University, Xi'an 710049, China*
[4]*Technische Universität Darmstadt Institut für Kernphysik, Schloßgartenstraße, Darmstadt 64289, Germany*

Correspondence should be addressed to Dong Wu; dwu.phys@sjtu.edu.cn

Received 25 June 2022; Revised 24 August 2022; Accepted 3 September 2022; Published 26 September 2022

Academic Editor: Dimitri Batani

Copyright © 2022 Xiaochuan Ning et al. This is an open access article distributed under the Creative Commons Attribution License, which permits unrestricted use, distribution, and reproduction in any medium, provided the original work is properly cited.

The proton-boron ($p\,^{11}B$) reaction is regarded as the holy grail of advanced fusion fuels, where the primary reaction produces 3 energetic α particles. However, due to the high nuclear bounding energy and bremsstrahlung energy losses, energy gain from the $p\,^{11}B$ fusion is hard to achieve in thermal fusion conditions. Owing to advances in intense laser technology, the $p^{11}B$ fusion has drawn renewed attention by using an intense laser-accelerated proton beam to impact a boron-11 target. As one of the most influential works in this field, Labaune et al. first experimentally found that states of boron (solid or plasma) play an important role in the yield of α particles. This exciting experimental finding rouses an attempt to measure the nuclear fusion cross section in a plasma environment. However, up to now, there is still no quantitative explanation. Based on large-scale, fully kinetic computer simulations, the inner physical mechanism of yield increment is uncovered, and a quantitative explanation is given. Our results indicate the yield increment is attributed to the reduced energy loss of the protons under the synergetic influences of degeneracy effects and collective electromagnetic effects. Our work may serve as a reference for not only analyzing or improving further experiments of the $p\,^{11}B$ fusion but also investigating other beam-plasma systems, such as ion-driven inertial confinement fusions.

1. Introduction

Progress in fusion experiments has been continuously made towards the final goal of contributing to the world's energy supply. Both the magnetic confinement fusion (MCF) experiments and the inertial confinement fusion (ICF) experiments have achieved significant milestones in recent years. The Experimental Advanced Superconducting Tokamak (EAST) at Hefei has made a world record for realizing a 101-second H-mode discharge [1], and the most advanced ICF experiments at the Livermore National Ignition Facility (NIF) have obtained a 1.35-MJ fusion energy output recently, which is about 70% of the laser input energy [2]. Despite the great achievements, there remains a long way to go to solve the energy crisis. For the magnetic confinement approach, adequate plasma confinement time and qualified materials for the first wall of the reactor, which can bear the tough conditions, are still two main issues to be addressed. As for the inertial confinement approach, in the case of the NIF, though it obtains 1.35-MJ energy, it starts with more than 400 MJ of total stored energy. From this perspective, the ratio of the total output energy to the total input energy is quite low and far from the envisioned goal of achieving a gain of 10. Moreover, 14-MeV neutrons produced by deuterium-tritium (D-T)

https://doi.org/10.1155/2022/9868807 Published online by Cambridge University Press

fusion also raise some concerns about induced radioactivity, and it is still a challenging problem to efficiently convert neutron energy into useful electricity.

While we are convinced that nuclear fusion is the world energy source of the future, it is obvious that even if, from now on, all fusion scenarios based on the ITER technology or similar technology proceed on schedule, fusion will not contribute significantly to eliminating the problems associated with climate change in a short time. Having said that, we believe that it makes sense to investigate fusion scenarios that use fusion fuel that is not radioactive and is available in abundant quantities. The holy grail of advanced fusion fuels, therefore, is considered to be the p ^{11} B reaction, where the primary reaction produces 3 energetic α particles.

$$^{11}B + p \longrightarrow 3\alpha + 8.7\,MeV. \tag{1}$$

Only secondary reactions produce neutrons and induce radioactivity. Although the peak fusion cross section is comparable to the D-T fusion, due to the much higher nuclear bounding energy and bremsstrahlung energy losses, energy gain from the p ^{11} B fusion is hard to achieve in thermal fusion conditions.

Owing to advances in laser technology [3, 4], it has becomes easier to obtain high-intensity ion beams [5, 6] and explore warm-dense-matter physics [7, 8] or high-energy-density physics [9, 10], and the p ^{11} B fusion has also drawn renewed attention [11–13]. The proposal of using intense laser beams or intense laser-accelerated proton beams to impact a boron target so as to generate the p ^{11} B fusion is becoming increasingly attractive. Based on this method, a number of groups [14–20] have performed a series of experiments on the p ^{11} B fusion reaction and measured the yields of α particles. Meanwhile, significant progress has also continuously been made in this field. The record yield of α particles has increased from 10^5/sr in 2005 [14, 21] to 10^{10}/sr in 2020 [18]. However, there still remain unclear physical mechanisms in the interaction of a proton beam and a boron target, which strongly depends on the intensity of the proton beam as well as the conditions of the boron target, including temperature, density, ingredients, and so on, and potentially has a large influence on the possibility of the p ^{11} B fusion reaction and the α-particle yield. Labaune et al. [15] first experimentally found that states of boron (solid or plasma) play an important role in the yield of α particles produced by the p ^{11} B fusion reaction. In their experiments, compared with boron solid, a boron plasma ablated by a nanosecond laser can produce many more (nearly two orders of magnitude more) α particles under the impact of a proton beam accelerated by a picosecond laser. As the inner physical mechanism of their experiments is still not clear, in order to figure out the issue, we have recently performed a set of simulations according to their experiments.

2. The Interaction between a Nanosecond Laser and a Boron Solid

To ascertain the specific state of the boron target after it is ablated, we have performed a one-dimensional radiation-hydrodynamic simulation with the MULTI-1D code [22] on the interaction of a nanosecond laser pulse and a boron solid, which is the first step in the experiment of Labaune et al. The MULTI-1D code has been widely used by various authors [23–27]. Readers are suggested to refer to Ref. [22] for more detailed information. In our simulation, the grid size is 8 μm and the time step is 0.02 ns. To be consistent with the experiments, the laser duration time is 1.5 ns with a 0.53 μm wavelength and an intensity of 6×10^{14}Wcm^{-2}. The initial mass density of the boron solid is set to 2.34 g/cm^3. The simulation results of the mass density distributions and the temperature distributions of the boron target at different moments are displayed in Figures 1(a) and 1(c). For the purpose of further analysis, we have extracted the data at $t = 1.2$ ns, as shown in Figures 1(b) and 1(d). A low-density boron plasma is widely formed in the region away from the boron solid, whereas, on the surface of the boron solid, there actually exists a high-density boron plasma that is driven by shocks. To the best of our knowledge, this high-density boron plasma was not considered seriously in previous studies. It can also be seen in Figures 1(b) and 1(d) that the surface high-density boron plasma is about 5 times denser than the boron solid, its range is about tens of microns, and its temperature is about 10 eV. Under this condition, the ionization degree of the boron target is about two [28]. To quantitatively evaluate the impact of degeneracy effects, we can define the degeneracy degree of plasma electrons as $\theta = k_B T_e / E_F$, where $k_B T_e$ is the thermal energy and $E_F = (3\pi^2 n_e)^{2/3} \hbar^2 / (2m_e)$ is the Fermi energy. Here, n_e is the density of plasma electrons, $\hbar$ is the reduced Planck's constant and m_e is the electron mass. By using the above parameters of the boron target, we can obtain.

$$\theta = \frac{k_B T_e}{E_F} = 0.23 < 1. \tag{2}$$

This indicates that after the laser ablated the boron solid, degeneracy effects indeed should be taken into account.

3. The Interaction Between a Proton Beam and a Boron Target under the Different States

Next, we further performed another set of simulations with the LAPINS code [29–33] on the p^{11}B fusion by injecting proton beams into a boron solid and a boron plasma, respectively. To make the simulations more credible and closer to the real experimental situation, modules of collisional effects [30], degeneracy effects [31] and nuclear reactions [32] are contained in the LAPINS code. Detailed information on these modules can be found in the relevant references. Moreover, to deal with the self-generated electromagnetic fields of the beam-target system, collective electromagnetic effects are also considered in the LAPINS code. As a hybrid PIC code, the LAPINS code treats plasma ions and the injected beam particles by using the traditional PIC method, while plasma electrons are treated as a fluid, of which the current density is solved by applying Ampere's law as follows [34]:

https://doi.org/10.1155/2022/9868807 Published online by Cambridge University Press

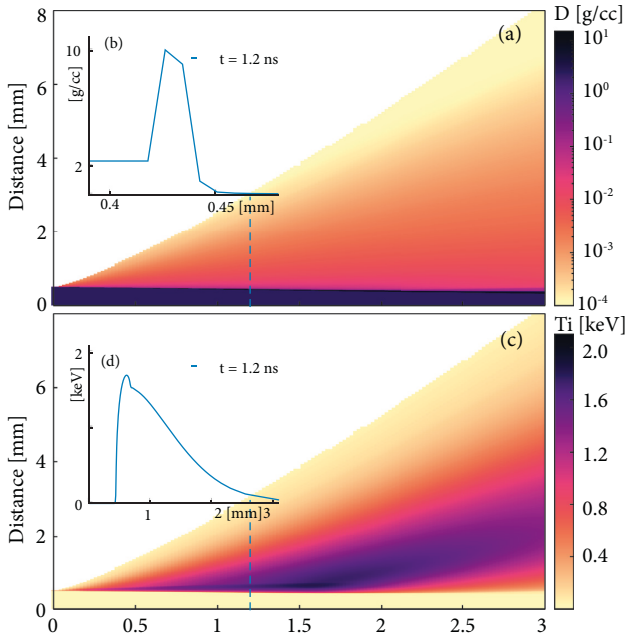


FIGURE 1: Evolution of the mass density distribution in (a) and the temperature distribution in (c) of boron ions with time. (b) and (d) correspond to the mass density distribution and the temperature distribution at $t = 1.2$ ns, respectively.

$$J_e = \frac{1}{2\pi}\nabla \times B - \frac{1}{2\pi}\frac{\partial E}{\partial t} - J_b - J_i, \tag{3}$$

where B is the magnetic field, E is the electric field, J_b is the beam current density and J_i is the plasma ion current density. Applying the continuity equation$\nabla \cdot J + \partial\rho/\partial t = 0$, where $J = J_b + J_e + J_i$ is the total current density, and ρ is the charge density, we can see that the Poisson's equation $\nabla \cdot E = 2\pi\rho$ is rigorously satisfied, which indicates the charge separation electric field is naturally contained in the LAPINS code.

When a charged particle beam is injected into a target, target electrons will quickly respond to the electromagnetic fields generated by the beam and neutralize the beam's charge and current. The fields generated by the beam-target system depend on not only the quality of the beam but also the target's ability to cancel the beam charge and current [34]. A widely used model to calculate the electric field is the basic Ohm's law [34–38], $E = \eta J_e$, where η is the resistivity, which is obtained by averaging over all binary collisions at each time step for each simulation cell in a natural manner. The LAPINS code applies to a more general form as follows:

$$E = \eta J_e - v_e \times B - \frac{1}{en_e}\nabla p_e, \tag{4}$$

where v_e is the flow velocity of plasma electrons, p_e is the plasma electron thermal pressure, n_e is the plasma electron density, and e is the elementary charge. The magnetic field is finally derived from Faraday's law,$\partial B/\partial t = -\nabla \times E$. As only a part of Maxwell's equations needs to be solved, this method is of high speed and particularly useful for large-scale simulations.

As mentioned above, degeneracy effects and collective electromagnetic effects are important in our cases. To evaluate the influences of these two effects on the p ^{11} B fusion, we have performed four simulations. With the module of collective electromagnetic effects on/off, a proton beam interacts with a boron solid/plasma. These simulations are based on a two-dimensional Z–Y Cartesian geometry. The grid size is 0.1 $\mu m\times$ 0.2 μm, and the time step is 1.6 fs. To make the proton beam possess a wide energy spectrum similar to the experimental result obtained by Labaune et al., we set both the kinetic energy and the temperature of the proton beam to 1 MeV. The duration time of the proton beam is 1 ps. The parameters of the boron targets are extracted from the results of the MULTI-1D simulation in Section 2. The density of the boron solid and the boron plasma is 2.34 g/cm ^{3} and 11.4 g/cm ^{3}, respectively. The temperature of the boron solid is set to 0.0243 eV (room temperature), and the temperature of the boron plasma is set to 10 eV. The simulation results of the proton mass density distributions and the electric field distributions at $t = 1.3$ ps are displayed in Figure 2.

4. Results and Discussion

Comparing Figures 2a and 2b, we can see that for the boron solid, the proton beam can only penetrate to the surface, whereas for the boron plasma, it can penetrate to a longer distance. This difference can be explained as follows. The boron solid has a large resistivity, and the boron plasma, with abundant free electrons, has a much lower resistivity. Ohm's law (4) reveals the fact that the large difference in resistivity will lead to a significant difference in the electric field generation. As shown in Figure. 2c and 2d, the maximum value of the electric field in the boron solid is more than 100 times stronger than that in the boron plasma. Such a strong electric field in the boron solid will greatly prevent the beam from penetrating deeper into the target.

Imitating the experimental measurement method, we have recorded the energy spectra of α particles escaping from the left simulation boundary in the range of 0 to 6.5 MeV, which are plotted in Figure 3. Comparing the cases of the boron plasma without electromagnetic fields (5N-noEB) and the boron solid without electromagnetic fields (N-noEB), we find that when electromagnetic fields are not calculated in the simulations, there are about 40% more α particles produced by the p^{11}B fusion reactions in the laser-ablated boron solid (boron plasma). This difference is attributed to degeneracy effects, which do not play a role in the solid boron target but become non-negligible after laser ablation, as mentioned above. A theoretical explanation can be given here. For degenerate electrons, their velocity distribution is governed by the Fermi-Dirac (FD) statistics as follows:

$$f_{FD}(v_e) = \frac{2m_e^3}{(2\pi\hbar)^3 n_e}\frac{1}{\exp[\beta(E_e - \mu)] + 1}, \tag{5}$$

where m_e is the electron mass, $\beta = 1/k_B T_e$, E_e is the electron energy, and μ is the chemical potential. The dielectric function of degenerate electrons can be expressed as [39].

https://doi.org/10.1155/2022/9868807 Published online by Cambridge University Press

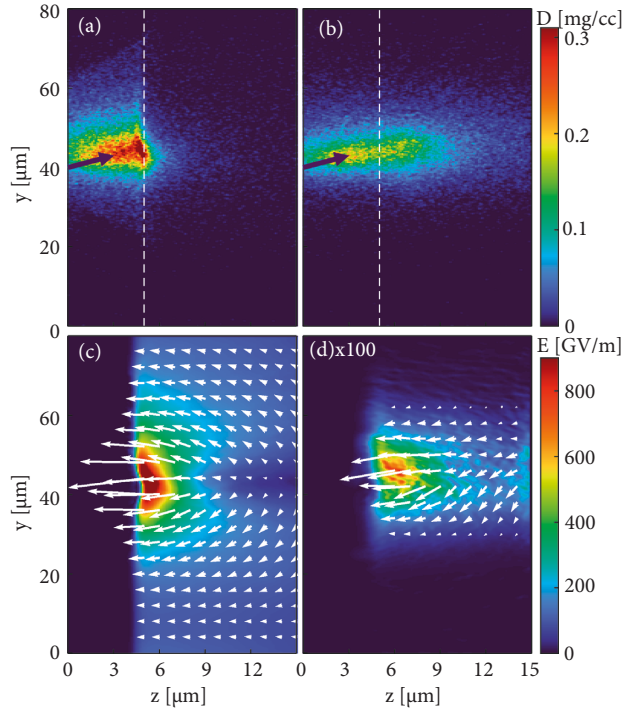


FIGURE 2: Mass density distributions of the proton beam and the electric field distributions at $t = 1.3$ ps for the boron solid in (a) and (c) and for the laser-ablated boron solid (boron plasma) in (b) and (d), respectively. The boron targets are located on the right side of the white dashed lines in (a) and (b). The black arrows in (a) and (b) indicate the incident direction of the proton beams, of which the angle is 45° to the z-axis. The white arrows in (c) and (d) are the directions of the electric fields. In (d), the white '×100' means the electric field is magnified by a factor of 100, which generally suggests the real electric field in (d) is at least 100 times weaker than that in (c).

$$\varepsilon(k,\omega) = 1 + \frac{1}{4\pi k_F a_0^2 z^3}[g(u+z) - g(u-z)]. \tag{6}$$

Here, a_0 is the Bohr radius, $k_F = m_e v_F \hbar = (3\pi^2 n_e)^{1/3}$, $u = \omega/kv_F$, $z = k/2k_F$, and

$$g(x) = \int_0^\infty \frac{y dy}{\exp\left(Dy^2 - \beta\mu\right) + 1} \ln\left(\frac{x+y}{x-y}\right), \tag{7}$$

where $D = E_F\beta$ is the degeneracy parameter. Finally, the stopping power of degenerate electrons can be obtained by the widely used dielectric formalism [40–43].

$$sp = -\frac{dE}{dz} = \frac{2(Ze)^2}{\pi v^2} \int_0^\infty \frac{dk}{k} \int_0^{kv} d\omega\omega \mathrm{Im}\left[\frac{-1}{\varepsilon(k,\omega)}\right]. \tag{8}$$

For the convenience of analysis, it is instructive to take advantage of the stopping power per unit density (SPPUD) to evaluate the influence of degeneracy effects

$$sp' = -\frac{sp}{n_e}. \tag{9}$$

Figure 4 shows the numerical results of (9) for different electron densities. It can be seen that if the electron density is

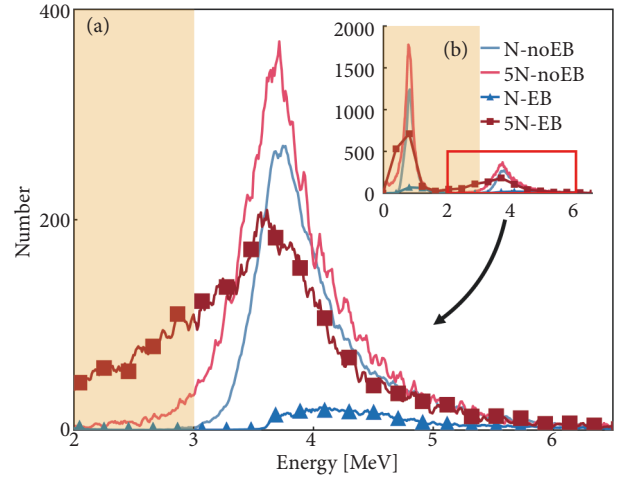


FIGURE 3: The energy spectra of α particles escaping from the left simulation boundary in the range of 0 MeV to 6.5 MeV: (1) the blue line (N-noEB), the boron solid without electromagnetic fields; (2) the red line (5N-noEB), the boron plasma without electromagnetic fields; (3) the blue triangle line (N-EB), the boron solid with electromagnetic fields; (4) the red square line (5N-EB), the boron plasma with electromagnetic fields. The yellow patch corresponds to where it cannot be measured in the experiments.

increased from 2.52×10^{23} cm^{-3} (density of the boron solid) to 1.26×10^{24} cm^{-3} (density of the boron plasma), SPPUD of the electrons is decreased. In our cases, the yield of α particles produced by the p ^{11} B fusion can be expressed as [18].

$$N_\alpha = \frac{3N_p n_e}{Z_i} \int_0^{E_0} \sigma(E)\left(\frac{dE}{dz}\right)^{-1} dE = \frac{3N_p}{Z_i} \int_0^{E_0} \frac{\sigma(E)}{sp'} dE, \tag{10}$$

where N_p is the number of protons, Z_i is the charge number of the boron ion, and$\sigma(E)$ is the cross section of the p ^{11} B fusion. (10) reveals the relation between the yield of α particles and the SPPUD of the electrons and implies that the proton beam propagating in the high-density boron plasma will have more chances to collide with boron nuclei, generate the p ^{11} B fusion and produce α particles, which is consistent with our simulation results about the gap between the cases of the boron plasma without electromagnetic fields (5N-noEB) and the boron solid without electromagnetic fields (N-noEB) in Figure 3. Both the theory and the simulations indicate that degeneracy effects have an influence on the p ^{11} B fusion. Nonetheless, quantitatively speaking, they are not the primary factor that causes the significant difference in the yield of α particles in the experiments of Labaune et al. since, as shown in Figure 3, they can only increase the yield by about 40%.

It can be seen in Figure 3 that there is a large gap between the cases of the boron solid without electromagnetic fields (N-noEB) and the boron solid with electromagnetic fields (N-EB), which indicates that in terms of the boron solid, collective electromagnetic effects have a huge influence on the number of fusion reactions and the yield of α particles. As mentioned above and shown in Figure 2c, when the

https://doi.org/10.1155/2022/9868807 Published online by Cambridge University Press

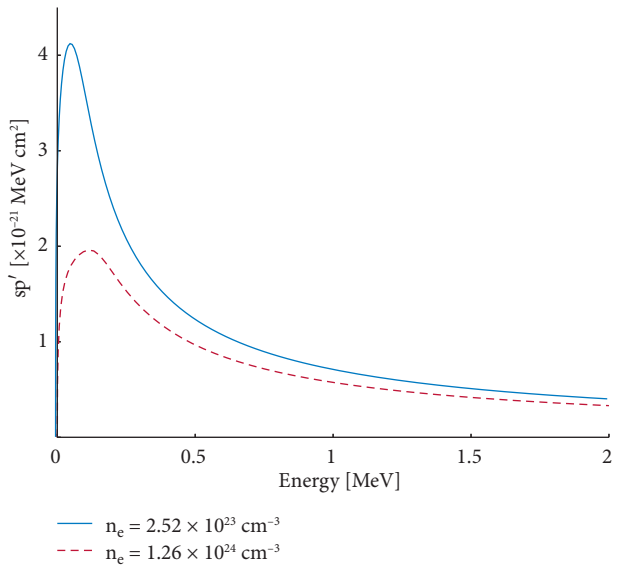


FIGURE 4: SPPUD as a function of the proton energy. For the blue solid line, the electron density is $n_e = 2.52 \times 10^{23}$ cm $^{-3}$, corresponding to the density of the boron solid, and for the red dotted line, the electron density is $n_e = 1.26 \times 10^{24}$ cm $^{-3}$, corresponding to the density of boron plasma.

proton beam is injected into the boron solid, a strong stopping electric field will be generated. On the one hand, it can greatly increase the energy loss of the proton beam and prevent the beam from penetrating. Recently, Ren et al. presented a piece of experimental evidence on the significantly enhanced energy loss of a laser-accelerated proton beam in the dense ionized matter [44], which is similar to the case we are describing. On the other hand, (10) shows that if the energy loss of the beam increases, the number of fusion reactions and the yield of α particles will decrease accordingly. For the boron plasma, the gap between the cases of the boron plasma without electromagnetic fields (5N-noEB) and the boron plasma with electromagnetic fields (5N-EB) is not that large because, compared with the boron solid, the boron plasma has a much lower resistivity and, according to Ohm's law Eq. (4), the generated electric field will also be smaller, as displayed in Figure 2c and 2d. Therefore, collective electromagnetic effects in the boron plasma are not as significant as in the boron solid. Collective electromagnetic effects described in this paper are a kind of nonlinear effects caused by a large number of injected ions. Previously commonly used single-particle theories and simulation models cannot be used here. Collective electromagnetic effects depend on many factors, such as the current density of the proton beam, the resistivity of the boron target, and the flow velocity of plasma electrons.

For the cases of the boron solid without electromagnetic fields (N-EB) and the boron plasma with electromagnetic fields (5N-EB), both degeneracy effects and collective electromagnetic effects are taken into account. The gap in the yields of α particles between these two cases is about a tenth of a second, which is in good agreement with the results at dt = 1.2 ns in the experiments of Labaune et al. As we have discussed above separately, the gap here originates from two aspects: degeneracy effects and collective electromagnetic effects. They exert influences on the number of fusion reactions by changing the energy loss of the proton beam. To be specific, the more energy the proton beam losses during its transport in boron targets, the smaller the number of fusion reactions between protons and boron atomic nuclei will be. Readers may notice that the specific numbers of recorded α particles in our simulations are greater than those in the experiments. Actually, it is caused by the difference in the total number of injected protons between our simulations and their experiments. As shown in Eq. (10), the yield of α particles produced by the p ^{11} B fusion is proportional to the number of protons. If the total numbers of protons in our simulations is greater than that in the experiments, then there will be an equal multiple difference in the yields of α particles. In this work, we are concerned with the difference in the α-particle yields produced in different states of boron targets rather than the specific numbers. From this perspective, our simulations are indeed in good agreement with the experiments.

Eventually, it should be mentioned that while α particles produced by the p ^{11} B fusion are propagating in boron targets, they are simultaneously heated and being stopped by the background particles [45–47], which, as a matter of fact, will alter the initial energy spectrum of α particles. This indicates that degeneracy effects and collective electromagnetic effects influence not only the yield of α particles but also their energy spectrum or velocity distributions. Degeneracy effects can be considered to be isotropic if local fluctuations of the boron density and temperature are ignored, but it is not the case with collective electromagnetic effects. For the α particles moving forward (the opposite direction of the electric field), their energy loss will be increased, whereas for the α particles moving backward (the same direction as the electric field), they will be accelerated by the electric field and gain energy. Whether one tries to use the p ^{11} B fusion to obtain a net energy output to solve the energy crisis or view the p^{11} B fusion as α-particle source, the influences of degeneracy effects and collective electromagnetic effects on the energy evolution of α particles could be a topic worthy of in-depth study in future work.

5. Conclusion

The influences of the boron state on the yield of α particles produced by the p ^{11} B fusion have been studied. It is found that compared with a boron solid, a boron plasma can produce much more α particles under the impact of a proton beam, which in this paper is proved to be attributed to degeneracy effects and collective electromagnetic effects. First, when a boron solid is ablated into a boron plasma by a nanosecond laser, degeneracy effects become non-negligible and can increase the yield of α particles by about 40%. Besides, a boron solid, as a poor conductor of electricity, has a large resistivity, while a boron plasma with abundant free electrons has a much lower resistivity. Ohm's law (4) indicates that such a transition from boron solid to a boron plasma will lead to a reduction in the generation of electromagnetic fields. Simulation results show that the

https://doi.org/10.1155/2022/9868807 Published online by Cambridge University Press

reduction of collective electromagnetic effects can significantly increase the yield of α particles by one to two orders of magnitude. Degeneracy effects and collective electromagnetic effects exert influences on the number of fusion reactions by changing the energy loss of the proton beam. To be specific, if the energy loss of the proton beam is decreased during its transporting in boron targets, the protons will have more chances to collide with boron nuclei, generate the p ^{11} B fusion, and produce α particles.

Our results are in good agreement with the experiments of Labaune et al., and we believe that for future experiments of the p ^{11} B fusion, a promising method to improve the yield of α particles is to heat and compress boron solid into a high-density plasma before injecting a proton beam, because in doing so, the energy loss of the proton beam will be reduced and, accordingly, more fusion reactions are expected to occur. Moreover, our findings may also be able to serve as a reference for investigating other beam-plasma systems, such as ion-driven inertial confinement fusions.

Data Availability

The data that support the findings of this study are available from the corresponding authors upon reasonable request.

Conflicts of Interest

The authors declare that there are no conflicts of interest.

Acknowledgments

This work was supported by the National Natural Science Foundation of China (Grant Nos. 12075204, 11875235 and 61627901), the Strategic Priority Research Program of Chinese Academy of Sciences (Grant no. XDA250050500) and Shanghai Municipal Science and Technology Key Project (No. 22JC1401500). Dong Wu thanks the sponsorship from Yangyang Development Fund. The authors thank Dr. Jinlong Jiao for his help in the radiation hydrodynamics simulations with the MULTI-1D code.

References

[1] B. N. Wan, Y. F. Liang, X. Z. Gong et al., "The EAST team, and Collaborators. Overview of EAST experiments on the development of high-performance steady-state scenario," *Nuclear Fusion*, vol. 57, Article ID 102019, 2017.

[2] D. Clery, "Laser-powered fusion effort near," *Science*, vol. 373, p. 841, 2021.

[3] C. N. Danson, C. Haefner, J. Bromage et al., "Petawatt and exawatt class lasers worldwide," *High Power Laser Science and Engineering*, vol. 7, p. e54, 2019.

[4] K. Burdonov, A. Fazzini, V. Lelasseux et al., "Characterization and performance of the apollon short-focal-area facility following its commissioning at 1 pw level," *Matter and Radiation at Extremes*, vol. 6, Article ID 064402, 2021.

[5] E. L. Clark, K. Krushelnick, J. R. Davies et al., "Measurements of energetic proton transport through magnetized plasma from intense laser interactions with solids," *Physical Review Letters*, vol. 84, no. 4, pp. 670–673, 2000.

[6] W. J. Ma, I. J. Kim, J. Q. Yu et al., "Laser acceleration of highly energetic carbon ions using a double-layer target composed of slightly underdense plasma and ultrathin foil," *Physical Review Letters*, vol. 122, no. 1, Article ID 014803, 2019.

[7] Z. Chen, X. Na, C. B. Curry et al., "Observation of a highly conductive warm dense state of water with ultrafast pump–probe free-electron-laser measurements," *Matter and Radiation at Extremes*, vol. 6, no. 5, Article ID 054401, 2021.

[8] R. Roycroft, P. A. Bradley, E. McCary et al., "Experiments and simulations of isochorically heated warm dense carbon foam at the Texas petawatt laser," *Matter and Radiation at Extremes*, vol. 6, no. 1, Article ID 014403, 2021.

[9] N. A. Tahir, C. Deutsch, V. E. Fortov et al., "Proposal for the study of thermophysical properties of high-energy-density matter using current and future heavy-ion accelerator facilities at gsi darmstadt," *Physical Review Letters*, vol. 95, no. 3, Article ID 035001, 2005.

[10] B. Y. Sharkov, D. H. H. Hoffmann, A. A. Golubev, and Y. T. Zhao, "High energy density physics with intense ion beams," *Matter and Radiation at Extremes*, vol. 1, no. 1, pp. 28–47, 2016.

[11] H. Hora, G. H. Miley, N. Azizi, B. Malekynia, M. Ghoranneviss, and X. T. He, "Nonlinear force driven plasma blocks igniting solid density hydrogen boron: laser fusion energy without radioactivity," *Laser and Particle Beams*, vol. 27, no. 3, pp. 491–496, 2009.

[12] H. Hora, G. H. Miley, M. Ghoranneviss, B. Malekynia, and N. Azizi, "Laser-optical path to nuclear energy without radioactivity: fusion of hydrogen–boron by nonlinear force driven plasma blocks," *Optics Communications*, vol. 282, no. 20, pp. 4124–4126, 2009.

[13] H. Hora, G. H. Miley, M. Ghoranneviss, B. Malekynia, N. Azizi, and X. T. He, "Fusion energy without radioactivity: laser ignition of solid hydrogen–boron (11) fuel," *Energy Environ. Sci.*vol. 3, no. 4, pp. 479–486, 2010.

[14] V. S. Belyaev, A. P. Matafonov, V. I. Vinogradov et al., "Observation of neutronless fusion reactions in picosecond laser plasmas," *Physical Review E - Statistical Physics, Plasmas, Fluids, and Related Interdisciplinary Topics*, vol. 72, no. 2, Article ID 026406, 2005.

[15] C. Labaune, C. Baccou, S. Depierreux et al., "Fusion reactions initiated by laser-accelerated particle beams in a laser-produced plasma," *Nature Communications*, vol. 4, no. 1, p. 2506, 2013.

[16] A. Picciotto, D. Margarone, A. Velyhan et al., "Boron-proton nuclear-fusion enhancement induced in boron-doped silicon targets by low-contrast pulsed laser," *Physical Review X*, vol. 4, no. 3, Article ID 031030, 2014.

[17] C. Baccou, S. Depierreux, V. Yahia et al., "New scheme to produce aneutronic fusion reactions by laser-accelerated ions," *Laser and Particle Beams*, vol. 33, no. 1, pp. 117–122, 2015.

[18] L. Giuffrida, F. Belloni, D. Margarone et al., "High-current stream of energetic alpha particles from laser-driven proton-boron fusion," *Physical Review E - Statistical Physics, Plasmas, Fluids, and Related Interdisciplinary Topics*, vol. 101, no. 1, 2020.

[19] D. Margarone, A. Morace, J. Bonvalet et al., "Generation of α-particle beams with a multi-kj, peta-watt class laser system," *Frontiers in Physiology*, vol. 8, p. 343, 2020.

[20] J. Bonvalet, P. Nicolai, D. Raffestin et al., "Energetic alpha-particle sources produced through proton-boron reactions by high-energy high-intensity laser beams," *Physical Review E -*

https://doi.org/10.1155/2022/9868807 Published online by Cambridge University Press

Statistical Physics, Plasmas, Fluids, and Related Interdisciplinary Topics, vol. 103, 2022.

[21] S. Kimura, A. Anzalone, and A. Bonasera, "Comment on "observation of neutronless fusion reactions in picosecond laser plasmas," *Physical Review E - Statistical Physics, Plasmas, Fluids, and Related Interdisciplinary Topics*, vol. 79, no. 3, Article ID 038401, 2009.

[22] R. Ramis, R. Schmalz, and J. Meyer-Ter-Vehn, "Multi — a computer code for one-dimensional multigroup radiation hydrodynamics," *Computer Physics Communications*, vol. 49, no. 3, pp. 475–505, 1988.

[23] J. Jiao, B. Zhang, J. Yu et al., "Generating high-yield positrons and relativistic collisionless shocks by 10 pw laser," *Laser and Particle Beams*, vol. 35, no. 2, pp. 234–240, 2017.

[24] M. Cipriani, S. Yu. Gus'kov, R. De Angelis et al., "Laser-supported hydrothermal wave in low-dense porous substance," *Laser and Particle Beams*, vol. 36, no. 1, pp. 121–128, 2018.

[25] F. Y. Wu, R. Ramis, Z. H. Li et al., "Numerical simulation of the interaction between Z-pinch plasma and foam converter using code MULTI (#18353)," *Fusion Science and Technology*, vol. 72, no. 4, pp. 726–730, 2017.

[26] B. Cui, Z. Fang, Z. Dai et al., "Nuclear diagnosis of the fuel areal density for direct-drive deuterium fuel implosion at the shenguang-ii upgrade laser facility," *Laser and Particle Beams*, vol. 36, no. 4, pp. 494–501, 2018.

[27] G. Rigon, B. Albertazzi, T. Pikuz et al., "Micron-scale phenomena observed in a turbulent laser-produced plasma," *Nature Communications*, vol. 12, no. 1, pp. 2679–9, 2021.

[28] T. A. Heltemes and G. A. Moses, "Badger v1. 0: a fortran equation of state library," *Computer Physics Communications*, vol. 183, no. 12, pp. 2629–2646, 2012.

[29] D. Wu, W. Yu, S. Fritzsche, and X. T. He, "High-order implicit particle-in-cell method for plasma simulations at solid densities," *Physical Review E - Statistical Physics, Plasmas, Fluids, and Related Interdisciplinary Topics*, vol. 100, no. 1, Article ID 013207, 2019.

[30] D. Wu, X. T. He, W. Yu, and S. Fritzsche, "Monte Carlo approach to calculate proton stopping in warm dense matter within particle-in-cell simulations," *Physical Review E - Statistical Physics, Plasmas, Fluids, and Related Interdisciplinary Topics*, vol. 95, no. 2, Article ID 023207, 2017.

[31] D. Wu, W. Yu, S. Fritzsche, and X. T. He, "Particle-in-cell simulation method for macroscopic degenerate plasmas," *Physical Review E - Statistical Physics, Plasmas, Fluids, and Related Interdisciplinary Topics*, vol. 102, no. 3, p. 033312, 2020.

[32] D. Wu, Z. M. Sheng, W. Yu, S. Fritzsche, and X. T. He, "A pairwise nuclear fusion algorithm for particle-in-cell simulations: weighted particles at relativistic energies," *AIP Advances*, vol. 11, no. 7, Article ID 075003, 2021.

[33] D. Wu, W. Yu, Y. T. Zhao, D. H. H. Hoffmann, S. Fritzsche, and X. T. He, "Particle-in-cell simulation of transport and energy deposition of intense proton beams in solid-state materials," *Physical Review E - Statistical Physics, Plasmas, Fluids, and Related Interdisciplinary Topics*, vol. 100, no. 1, Article ID 013208, 2019.

[34] H. Cai, X. Yan, P. Yao, and S. Zhu, "Hybrid fluid-particle modeling of shock-driven hydrodynamic instabilities in a plasma," *Matter and Radiation at Extremes*, vol. 6, Article ID 035901, 2021.

[35] J. R. Davies, "Electric and magnetic field generation and target heating by laser-generated fast electrons," *Physical Review E - Statistical Physics, Plasmas, Fluids, and Related Interdisciplinary Topics*, vol. 68, no. 5, Article ID 056404, 2003.

[36] A. R. Bell, J. R. Davies, and S. M. Guerin, "Magnetic field in short-pulse high-intensity laser-solid experiments," *Physical Review E - Statistical Physics, Plasmas, Fluids, and Related Interdisciplinary Topics*, vol. 58, no. 2, pp. 2471–2473, 1998.

[37] J. R. Davies, J. S. Green, and P. A. Norreys, "Electron beam hollowing in laser–solid interactions," *Plasma Physics and Controlled Fusion*, vol. 48, no. 8, pp. 1181–1199, 2006.

[38] A. P. L. Robinson, M. H. Key, and M. Tabak, "Focusing of relativistic electrons in dense plasma using a resistivity-gradient-generated magnetic switchyard," *Physical Review Letters*, vol. 108, no. 12, Article ID 125004, 2012.

[39] P. Norreys, D. Batani, S. Baton et al., "Fast electron energy transport in solid density and compressed plasma," *Nuclear Fusion*, vol. 54, no. 5, Article ID 054004, 2014.

[40] R. Néstor, "Arista and Werner Brandt. Dielectric response of quantum plasmas in thermal equilibrium," *Physical Review A*, vol. 29, pp. 1471–1480, 1984.

[41] R. Néstor, "Arista and Werner Brandt. Energy loss and straggling of charged particles in plasmas of all degeneracies," *Physical Review A*, vol. 23, 1981.

[42] M. D. Barriga-Carrasco, "Applying full conserving dielectric function to the energy loss straggling," *Laser and Particle Beams*, vol. 29, no. 1, pp. 81–86, 2011.

[43] D. Casas, A. A. Andreev, M. Schnürer, M. D. Barriga-Carrasco, R. Morales, and L. González-Gallego, "Stopping power of a heterogeneous warm dense matter," *Laser and Particle Beams*, vol. 34, no. 2, pp. 306–314, 2016.

[44] C. F. Clauser and N. R. Arista, "Stopping power of dense plasmas: the collisional method and limitations of the dielectric formalism," *Physical Review E - Statistical Physics, Plasmas, Fluids, and Related Interdisciplinary Topics*, vol. 97, no. 2, Article ID 023202, 2018.

[45] J. Ren, Z. Deng, W. Qi et al., "Observation of a high degree of stopping for laser-accelerated intense proton beams in dense ionized matter," *Nature Communications*, vol. 11, no. 1, p. 5157, 2020.

[46] P. S. Ray and H. Hora, "On thermalisation of energetic charged particles in fusion plasma with quantum electrodynamic considerations," *Zeitschrift für Naturforschung A*, vol. 32, no. 6, pp. 538–543, 1977.

[47] B. Malekynia, M. Ghoranneviss, H. Hora, and G. H. Miley, "Collective alpha particle stopping for reduction of the threshold for laser fusion using nonlinear force driven plasma blocks," *Laser and Particle Beams*, vol. 27, no. 2, pp. 233–241, 2009.

[48] B. Malekynia, H. Hora, N. Azizi et al., "Collective stopping power in laser driven fusion plasmas for block ignition," *Laser and Particle Beams*, vol. 28, no. 1, pp. 3–9, 2010.

https://doi.org/10.1155/2022/9868807 Published online by Cambridge University Press